Scientific Research Publishing

Journal of Geoscience and Environment Protection, 2026, 14(7), 465-480
https://www.scirp.org/journal/gep
ISSN Online: 2327-4344
ISSN Print: 2327-4336

Comparative Stability Analysis of Slopes in Gouache (West-Cameroon) Using Finite Element and Limit Equilibrium Methods

Willy Chance Guimezap Kenou[1*], Bertile Ilalie Manefouet[2], Thierry Constant Nie Noumsi[3], Vladimir Willianov Keubou Tatapzia[1,2], François Ngapgue[3], Ulrich Audrey Kamdem Dassi[2]

[1]Pôle de Recherche de l'Inovation et de l'Entreprenariat (PRIE), Institut Universitaire de la côte, Douala, Cameroon
[2]Faculty of Sciences, University of Dschang, Dschang, Cameroon
[3]Department of Civil Engineering, FOTSO Victor University Institute of Technology, University of Dschang, Bandjoun, Cameroon
Email: *willychance@gmail.com

How to cite this paper: Guimezap Kenou, W. C., Manefouet, B. I., Nie Noumsi, T. C., Keubou Tatapzia, V. W., Ngapgue, F., & Kamdem Dassi, U. A. (2026). Comparative Stability Analysis of Slopes in Gouache (West-Cameroon) Using Finite Element and Limit Equilibrium Methods. *Journal of Geoscience and Environment Protection, 14,* 465-480.
https://doi.org/10.4236/gep.2026.147026

Received: April 8, 2026
Accepted: July 28, 2026
Published: July 31, 2026

Abstract

This study investigates the stability of three slopes in the Gouache area and its surroundings using both the Finite Element Method (FEM) and Limit Equilibrium Methods (LEM) to enable comparative analysis and potential design of slope reinforcement. Stability analyses were conducted based on the Mohr-Coulomb model and the reduced C-φ approach, with field and laboratory work undertaken to determine the necessary geotechnical parameters. The studied slopes are characterized by significant heights (exceeding 15 m) and moderately steep inclinations (over 40˚). Laboratory analyses show an average fine fraction of 51.81%, a liquid limit of 54.18%, a plastic limit of 35.58%, and a plasticity index of 18.6%. The optimal water content is 19% with a corresponding dry density of 1.66 g/cm^3 at Proctor optimum, and an average CBR index of 2.53%. According to Casagrande's plasticity chart, the soils at point 1 of slope 1 are classified as low-plasticity silts, while point 2 of slope 1 and slopes 2 and 3 are high-plasticity silts. HRB classification identifies all soils as clayey. The soils are over-consolidated with an average cohesion of 43.33 kPa and an internal friction angle of 32.28˚. Stability coefficients obtained using Plaxis are 1.460, 3.815, and 3.146 for slopes 1, 2, and 3, with maximum displacements of 0.335 m, 26.48 m, and 15.85 m, respectively. Limit Equilibrium analyses using Geo-Studio yield factors of safety for slope 1 ranging from 0.939 to 0.997 depending on the method, for slope 2 from 2.125 to 2.177, and for slope 3 from 1.654 to 1.702. These results indicate that slope 1 is unstable and potentially hazardous, whereas slopes 2 and 3 are stable.

Keywords

Embankment, Safety Coefficient, Stabilization, Finite Element Methods, Limit Equilibrium Methods, C-φ Reduction

1. Introduction

Mass movements represent one of the most damaging natural hazards in mountainous regions due to their significant human, economic, and infrastructural impacts. They are defined as the downslope displacement of soil and/or rock masses along a failure surface under the effect of gravity and occur in several forms, among which landslides are particularly destructive (Tahar & Mouatez, 2023; Kusumajaya et al., 2023). In developing countries, rapid and often unplanned urbanization increases population vulnerability to such hazards, particularly through the occupation of geomorphologically unstable areas (Tsoata et al., 2020). In Bafoussam (West Cameroon), accelerated demographic growth has led to the expansion of settlements on unstable slopes, as illustrated by the deadly landslide that occurred in the Gouache area in October 2019, highlighting the pronounced instability of local cut slopes.

Slope stability analysis is a key tool for understanding and preventing landslides. It primarily relies on the evaluation of the factor of safety using analytical approaches, such as limit equilibrium methods, and numerical techniques, notably the finite element method. Although these methods have proven effective, their comparative application remains limited in certain geographical contexts, particularly in sub-Saharan Africa. Recent studies conducted in Gouache and its surroundings have focused on landslide susceptibility mapping using multicriteria analyses that incorporate morphometric and environmental factors. However, these approaches mainly address spatial susceptibility and do not explicitly account for the mechanical instability of slopes, which plays a decisive role in landslide initiation (Tsoata et al., 2020; Zangmene et al., 2023). This study aims to bridge this gap by conducting a comparative analysis of slope stability in Gouache and its surrounding areas using both limit equilibrium and finite element methods. The objectives are to assess the factor of safety of selected slopes, characterize the mechanical properties of *in-situ* materials, and propose appropriate stabilization measures, thereby contributing to a better understanding of slope failure mechanisms and to the mitigation of landslide risk in a rapidly expanding urban environment.

2. Methodology

2.1. Location of Study Area

The study area is located in the West Region of Cameroon (**Figure 1**), within the Bafoussam III Subdivision, Mifi Division, with Bamougoum as its administrative headquarters. It is bordered to the south by the municipalities of Bamendjou (Hauts-Plateaux Division) and Pete-Bandjoun (Koung-Khi Division), to the west by Penka-Michel (Menoua Division), to the north by Bafoussam II and Mbouda (Bamboutos Division), and to the east by Bafoussam I, all within the Mifi Division. Geographically, the study area extends between latitudes 05˚27'00"N and 05˚30'00"N, and longitudes 10˚22'00"E and 10˚24'00"E.

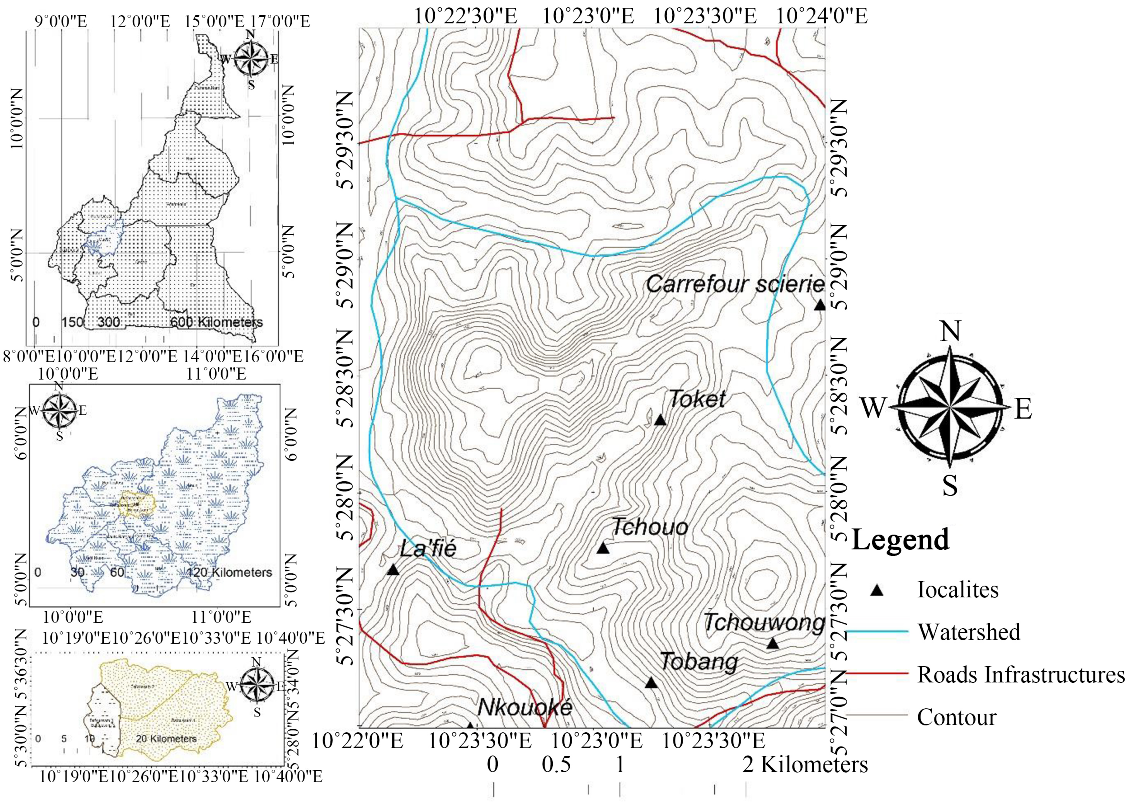

Figure 1. Topographic map of the study area.

2.2. Soil Sampling

Field investigations included geological reconnaissance, slope delineation, and soil sampling. A representative natural slope was selected, and its geometry (height and inclination) was measured using a clinometer and reference stakes. Two types of soil samples were collected at mid-slope (B horizon):

- Disturbed samples: 50 kg from four points for classification tests.
- Undisturbed samples: Extracted using PVC core samplers (10 cm diameter, 20 cm height) for mechanical testing, sealed with paraffin to preserve moisture.

2.3. Laboratory Testing

Laboratory tests determined the physical, mechanical, and index properties of the soil, following French (NF) and/or Cameroonian (BNQ) standards.

Identification tests:

- Natural water content (oven drying at 105˚C) (NF P94-050, 1995);

- Particle size distribution (sieving and sedimentation) (NF P94-056, 1996);
- Atterberg limits (Casagrande method) and derived plasticity and consistency indices (NF P94-051);
- Specific gravity (pycnometer method) (NF P94-054, 1991).

Mechanical and compaction tests:

- Standard Proctor compaction (OMC and MDD) (NF P94-093);
- California Bearing Ratio (CBR) on soaked and compacted specimens (NF P94-078);
- Direct shear test for cohesion (c) and internal friction angle (φ) (NF P94-071-1, 1994);
- Oedometer test for compressibility parameters (compression index Cc) (NF P94-090-1, 1994);
- recompression index (Cr), preconsolidation pressure (σ'_P).

2.4. Soil Classification

Soils were classified using: HRB (Highway Research Board), and LCPC (France) systems based on grain size and plasticity.

2.5. Slope Stability Analysis

Slope stability was assessed using two complementary approaches:

- **Limit Equilibrium Method (LEM):** Performed in GeoStudio Slope/W using the Mohr-Coulomb model. Various slip surface search algorithms and methods (Bishop Simplified, Spencer, Morgenstern-Price) were applied. The minimum factor of safety (FS) was identified for the critical slip surface.
- **Finite Element Method (FEM):** Implemented in PLAXIS 2D. The slope geometry was discretized, and the Mohr-Coulomb model was assigned. Initial stresses were generated via the (K0) procedure. Phi-c reduction analysis was performed to determine the FS, which was then compared to the LEM results.

3. Results

3.1. Field Investigations

3.1.1. Morphological and Structural Description of Soil Profiles

Four soil profiles were described in the field (**Figure 2**). Profiles 1 and 2 correspond to Slope 1 at Gouache, the site of the 2019 landslide, while Profiles 3 and 4 were observed on Slopes 2 and 3 in the surrounding areas. Profiles 3 and 4 show zones affected by water infiltration.

➢ **Soil Profile 1** (N 05˚29'11.3", E 010˚22'6.9"; altitude 1342 ± 3 m) is located in a cultivated area. It consists of:
  - Horizon A (0 - 50 cm): fine, pedotubed soil, pale red (7.5 R 6/2), clay-sandy texture, granular structure, with millimetric roots and rootlets. The boundary with the underlying horizon is regular and gradual (**Figure 2**).
  - Horizon B (50 - 90 cm): mineral horizon, light red (2.5 YR 6/6), massive structure, with rootlets and whitish-reddish spots.

- **Soil Profile 2** (N 05˚29'07.2", E 010˚22'32"; altitude 1350 ± 6 m), located at the landslide core, comprises:
  - Horizon A (0 - 72 cm): fine, pedotubed soil, dark reddish black (7.5 YR 2.5/1), clay-silty-sandy texture, granular structure, with fine roots and rootlets. The boundary with the underlying horizon is irregular and gradual (**Figure 2**).
  - Horizon B (72 - 210 cm): mineral horizon, red (10 R 5/8), clay-sandy texture, massive structure.
- **Soil Profile 3** (N 05˚29'04.1", E 010˚22'06.4"; altitude 1314 ± 3 m) consists of:
  - Horizon A (0 - 20 cm): fine, pedotubed soil, dark reddish black (7.5 R 2.5/1), clay-sandy texture, granular structure, with roots and rootlets. The boundary with the underlying horizon is regular and gradual (**Figure 2**).
  - Horizon B (20 - 180 cm): mineral horizon, dark red (2.5 YR 3/6), clay-sandy texture, massive structure.
- **Soil Profile 4** (N 05˚28'43.56", E 010˚22'23.64"; altitude 1389 ± 3 m) includes:
  - Horizon A (0 - 47 cm): fine, pedotubed soil, dark grayish black (5 R 4/1), clay-sandy texture, massive structure, with rock fragments and roots. The boundary with the underlying horizon is irregular and gradual (**Figure 2**).
  - Horizon B/C (47 - 130 cm): mineral horizon, yellowish-red (5 YR 5/8), with C phase embedded within B.

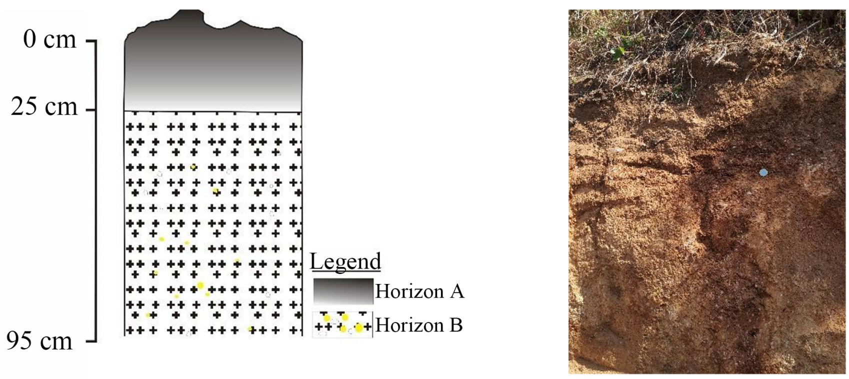

Soil Profile 1

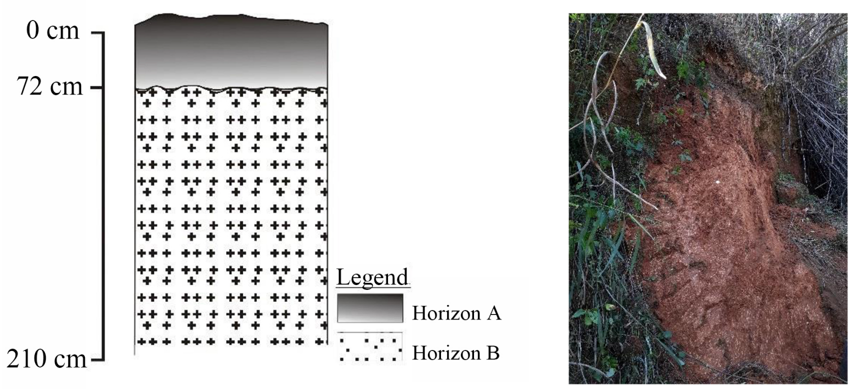

Soil Profile 2

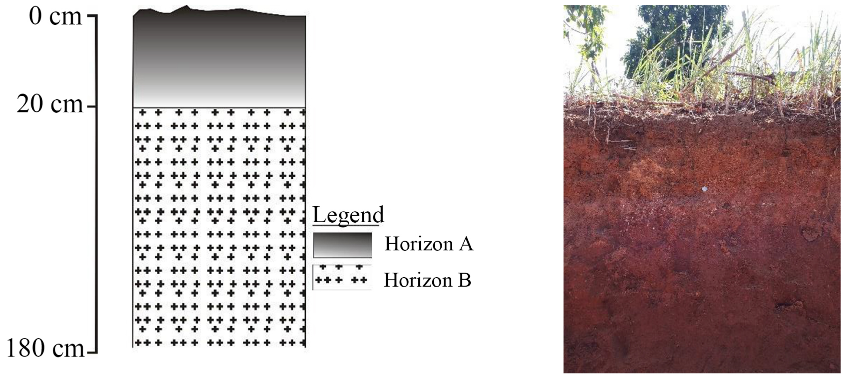

Soil Profile 3

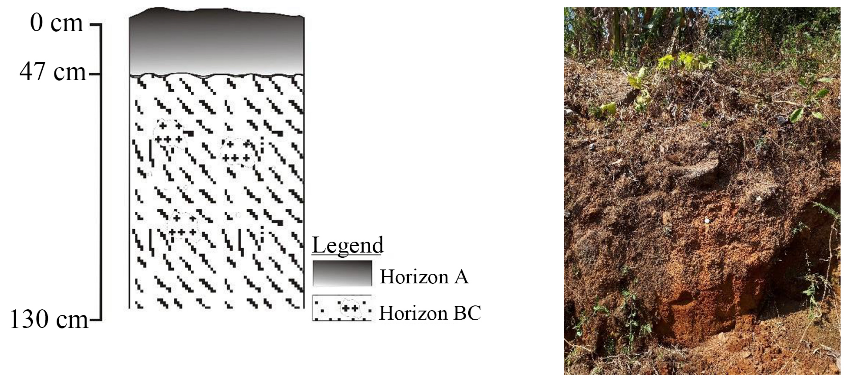

Soil Profile 4

Figure 2. Soils profile.

3.1.2. Geometrical Characteristics of the Slopes

The geometrical properties of the three studied slopes were determined, including slope height (H), inclination angle relative to the horizontal (β), and horizontal distance (D). The results show that, Slope 1 (Profiles 1 and 2) exhibits a height of 30.44 m, an inclination of 59˚, and a horizontal distance of 18.29 m. Slope 2 (Profile 3) has a height of 25 m, slope angle of 52˚, and horizontal distance of 19.53 m, while Slope 3 (Profile 4) shows a height of 26.38 m, slope angle of 48˚, and horizontal distance of 23.76 m. The average values for the three slopes are H = 27.27 m, β = 53˚, and D = 20.52 m.

3.2. Laboratory Results

3.2.1. Physical Properties

1) Natural Water Content, Specific Gravity, and Atterberg Limits

The physical properties of the soil, including natural water content (W), specific gravity, and Atterberg limits (Figure 3), were determined to characterize the materials. The results are summarized in Table 1. Natural water content ranged from 11.13% (Sample 1) to 23.47% (Sample 4), with an average of 16.7%. The liquid limit (WL) (Figure 3), varied between 44% and 58.2%, while the plastic limit (WP) ranged from 29.37% to 42.85%. The plasticity index (Ip) and consistency index

(Ic)) averaged 18.6 and 2.11, respectively. The absolute density of solids ranged from 2.27 to 2.45 g/cm³, with a mean value of 2.35 g/cm³.

Table 1. Physical properties of soil samples.

Samples	W (%)	WL (%)	WP (%)	Ip	Ic	Specific gravity (g/cm³)
Sample 1	11.13	44.0	29.37	14.63	2.25	2.33
Sample 2	19.22	56.4	33.33	23.07	1.61	2.36
Sample 3	12.98	58.2	42.85	15.35	2.95	2.45
Sample 4	23.47	58.1	36.75	21.35	1.62	2.27
Maximum	23.47	58.2	42.85	23.07	2.95	2.45
Minimum	11.13	44.0	29.37	14.63	1.61	2.27
Average	16.7	54.18	35.58	18.6	2.11	2.35

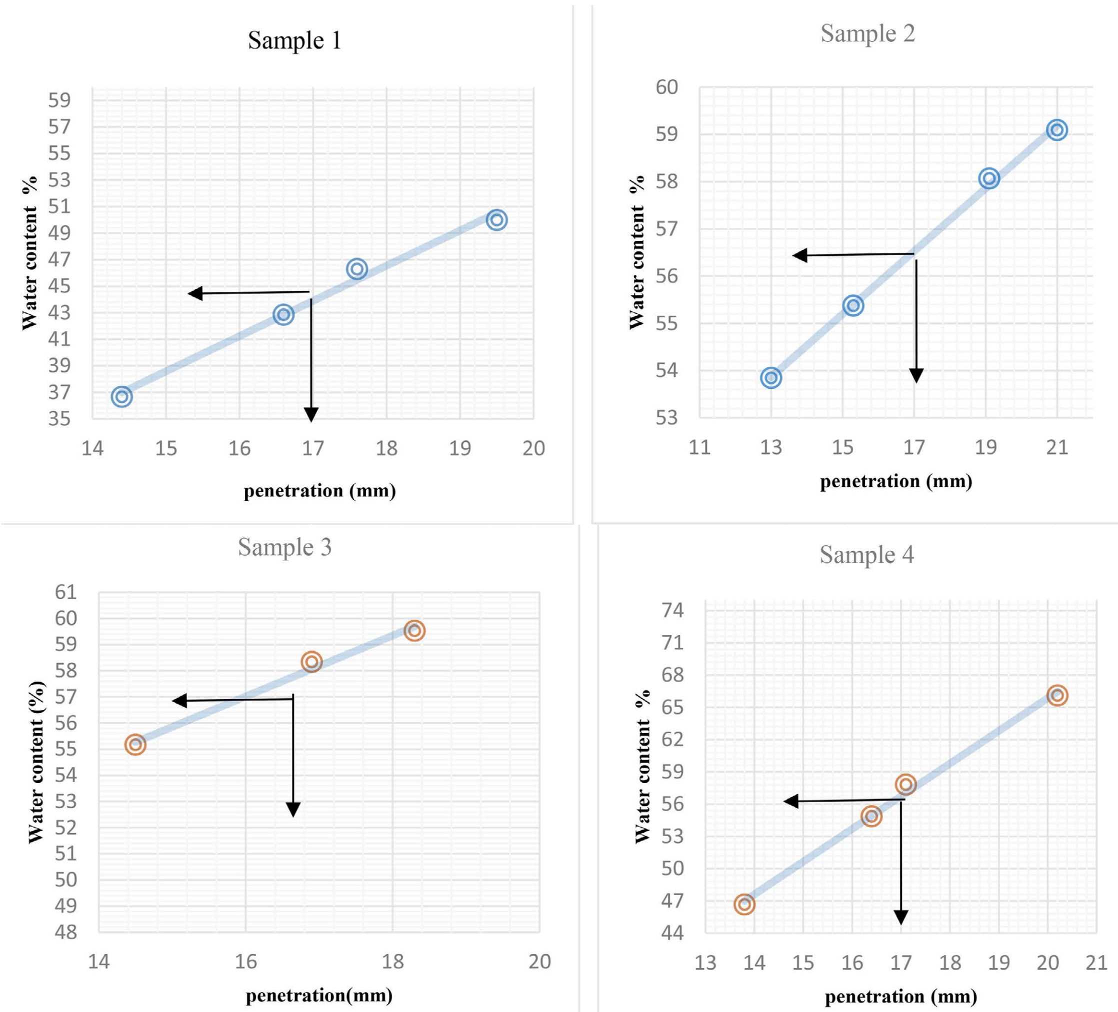

Figure 3. Liquid limit curve.

2) Particle Size Distribution

The particle size distribution of the soil samples was determined by sieve analysis, and the results were used to construct the grain size curves shown in Figure 4. The curves represent cumulative percentages of soil passing through the sieves as a function of sieve diameter, providing a clear indication of the soil texture and grading for each sample. These distributions help characterize the relative proportions of sand, silt, and clay, which are key parameters for assessing slope stability and mechanical behaviour.

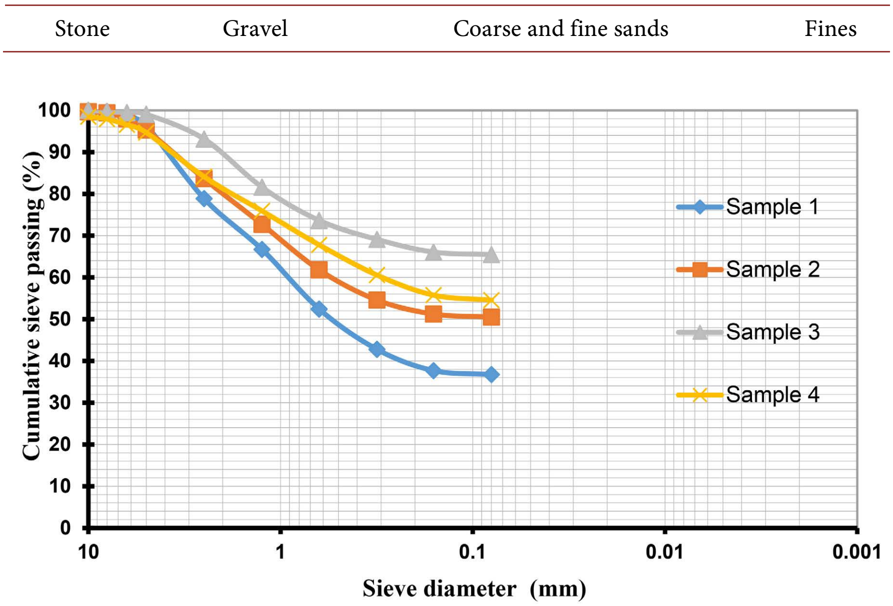

Figure 4. Grain size distribution curves of the different sample.

The particle size composition of the four soil samples (Sample 1 - Sample 4) is summarized in Table 2. Gravel content varied from 21.13% (Sample 1) to 57.24% (Sample 4), sand content ranged from 42.12% (Sample 1) to 66.70% (Sample 2), and fine particles (silt + clay) ranged from 36.75% (Sample 1) to 65.45% (Sample 3). On average, the soil samples contained 39.81% gravel, 51.01% sand, and 51.81% fines. These variations reflect the heterogeneity of soil texture across the slopes, which has important implications for slope stability and mechanical behavior.

Table 2. Particle size composition of soil samples (%).

Sample	Gravel (%)	Sand (%)	Fines (%)
Sample 1	21.13	42.12	36.75
Sample 2	33.30	66.70	50.51
Sample 3	47.56	52.44	65.45
Sample 4	57.24	42.76	54.55
Minimum	21.13	42.12	36.75
Maximum	57.24	66.70	65.45
Average	39.81	51.01	51.81

3.2.2. Mecaniques Parameters

1) Proctor Test Parameters

The Standard Proctor compaction test results for the soil samples (Figure 5) are summarized in Table 3. The optimum moisture content (w*opt)* ranged from 17% (Sample 2) to 20.4% (Sample 4), with an average of 19%. The corresponding maximum dry density *(*$\gamma_{d\max}$) varied from 1.61 g/cm^3 (Sample 4) to 1.72 g/cm^3 (Sample 1), with an average of 1.66 g/cm^3. These results reflect the compaction characteristics of the soils, which are essential for understanding their mechanical behavior and assessing slope stability.

Table 3. Proctor test results.

Sample	Sample 1	Sample 2	Sample 3	Sample 4	Average
w(opt) (%)	19	17	19.6	20.4	19
$\gamma_{d\max}$ (g/cm^3)	1.72	1.64	1.66	1.61	1.66

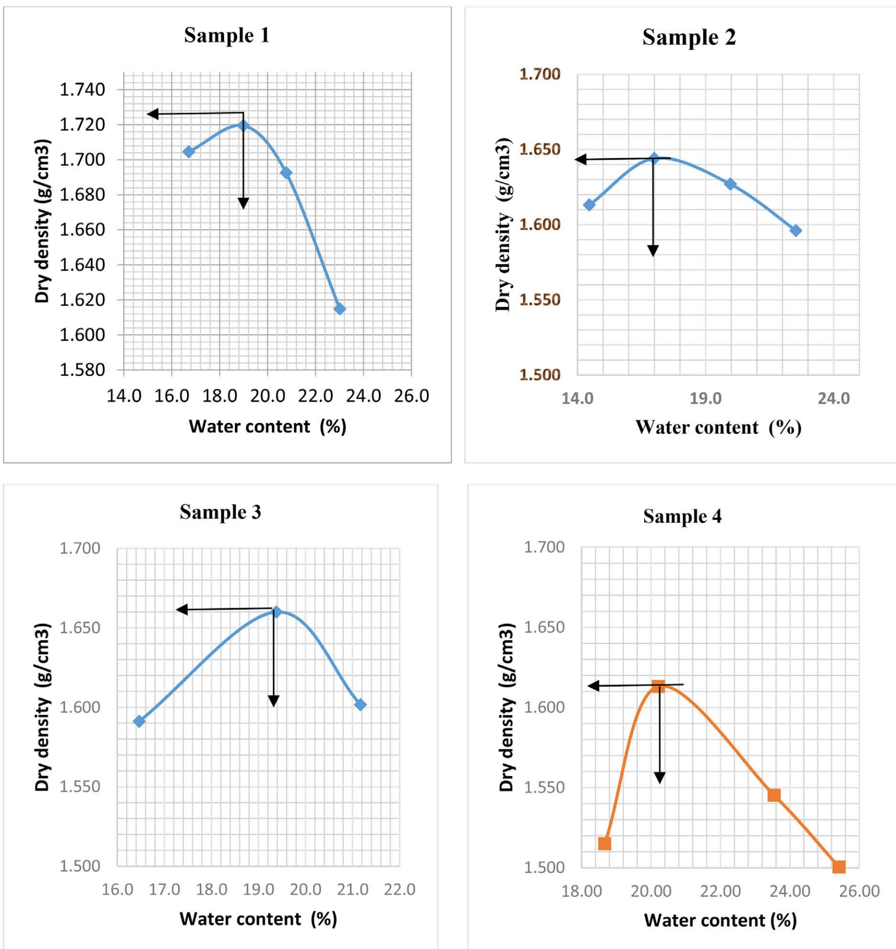

Figure 5. Proctors curves of soils samples E1 at E4.

2) California Bearing Ratio (CBR)

The California Bearing Ratio (CBR) tests were performed on soil samples compacted at 95% of the optimum moisture content. The results, summarized in Table 4, show that CBR values range from 0.41% (sample 2) to 5.97% (sample 1), with an average of 2.53%. These low CBR values indicate weak subgrade strength, highlighting the potential need for soil improvement or stabilization measures to ensure slope stability and support civil infrastructure.

Table 4. CBR values of soil samples at 95% OMC.

Sample	Sample 1	Sample 2	Sample 3	Sample 4	Average
CBR (%)	5.97	0.41	1.45	2.29	2.53

3) Oedometer Test Results

The oedometer tests were conducted on the soil samples to evaluate their compressibility and consolidation characteristics. The results are summarized in Table 5. The compression index (Cc) varied from 0.14 (sample 4) to 0.22 (sample 3), with an average of 0.18, while the recompression index (Cr) ranged from 0.02 (sample 4) to 0.05 (sample 3), averaging 0.031. The preconsolidation pressure (σ'p) ranged from 3.30 kPa (sample 1, sample 3) to 3.40 kPa (sample 4), with a mean of 3.32 kPa. The initial vertical effective stress (σ'v0) varied between 2.40 kPa (E1) and 3.33 kPa (E4), averaging 2.75 kPa. The overconsolidation ratio (OCR) ranged from 1.02 (sample 4) to 1.33 (sample 1), with an average of 1.22. The initial void ratio (e0) varied from 1.18 (sample 1) to 1.48 (sample 2), with a mean of 1.39. These parameters indicate the soil's potential for compression under applied loads, which is critical for slope stability and foundation design.

Table 5. Oedometer test results.

Samples	Sample 1	Sample 2	Sample 3	Sample 4	Average
Cc	0.15	0.20	0.22	0.14	0.18
Cg	0.028	0.027	0.05	0.02	0.031
σ'p (kPa)	3.3	3.39	3.30	3.40	3.32
σv0' (kPa)	2.4	2.68	2.58	3.33	2.75
Roc	1.33	1.26	1.28	1.02	1.22
e0	1.18	1.48	1.46	1.45	1.39

eo: initial void ratio; **Cc**: compression index; **Cg**: swelling index; **σ'vo**: initial vertical effective stress; **σ'p**: preconsolidation pressure; Roc: overconsolidation ratio.

4) Direct Shear Test Results

Direct shear tests were performed on the soil samples to determine their shear strength parameters. The results are summarized in Table 6. The cohesion (C) values ranged from 18.22 kPa (Sample 1) to 70.44 kPa (Sample 3), with an average of 43.33 kPa. The internal friction angle (φ) varied between 28.74˚ (Sample 4) and 36.7˚ (Sample 3), with a mean value of 32.28˚. These parameters are critical for evaluating slope stability and designing soil reinforcement measures.

Table 6. Shear strength parameters of soil samples.

Sample	Sample 1	Sample 2	Sample 3	Sample 4	Average
Cohesion C (kPa)	18.22	29.84	70.44	54.8	43.33
Internal friction angle φ (˚)	32.20	31.5	36.7	28.74	32.28

3.2.3. Soil Classification

The tested soils were classified according to two common geotechnical systems: the Highway Research Board (HRB) system and the Laboratoire Central des Ponts et Chaussées (LCPC) system. The results are presented in Table 7. According to HRB classification, sample 1 is classified as A-7-6, while samples 2, 3, and 4 are classified as A-7-5. Using the LCPC system, all samples are identified as silty sands (SL). These classifications reflect the fine-grained, silty-sandy nature of the soils, which is consistent with the physical and mechanical properties obtained from laboratory tests.

Table 7. Soil classification results.

Sample	HRB	LCPC
Sample 1	A-7-6	Silty Sand (SL)
Sample 2	A-7-5	Silty Sand (SL)
Sample 3	A-7-5	Silty Sand (SL)
Sample 4	A-7-5	Silty Sand (SL)

3.3. Slope Stability Analysis

3.3.1. Limit Equilibrium Method (LEM)

Slope stability was evaluated using the Limit Equilibrium Method (LEM) under different assumptions, including Bishop (Figure 4), Morgenstern-Price, Spencer, Janbu, and Fellenius. These approaches allow identification of the critical slip surface and the corresponding Factor of Safety (FS) for each slope. Slope 1 corresponds to the average cohesion and friction angle of soil profiles 1 and 2. Table 8 presents the FS values under dry conditions, while Table 9 shows the FS under a defined piezometric water level (Table 9). Results indicate that slope 1 has FS values close to 1, suggesting marginal stability, whereas slope 2 shows higher FS values, indicating greater stability. Slope 3 exhibits intermediate stability.

Table 8. Factor of safety of slopes under dry conditions (LEM).

Slope	Height (m)	Cohesion (kPa)	Friction angle φ (˚)	Unit weight (kPa/cm³)	Fs (Ordinary)	Fs (Bishop)	Fs (Janbu)	Fs (Spencer)	Fs (Morgenstern-Price)
1	30.44	24.03	31.85	15.79	0.965	0.997	0.939	0.967	0.966
2	25	70.44	36.7	15.96	2.125	2.173	2.135	2.177	2.173
3	26.38	54.8	28.74	15.21	1.655	1.701	1.654	1.702	1.698

Table 9. Factor of safety of slopes under piezometric water level (LEM).

Slope	Height (m)	Cohesion (kPa)	Friction angle φ (˚)	Unit weight (kPa/cm³)	Fs (Ordinary)	Fs (Bishop)	Fs (Janbu)	Fs (Spencer)	Fs (Morgenstern-Price)
1	30.44	24.03	31.85	15.79	0.840	0.764	0.760	0.760	0.761
2	25	70.44	36.7	15.96	1.867	1.773	1.742	1.781	1.770
3	26.38	54.8	28.74	15.21	1.442	1.395	1.360	1.398	1.395

These results show that piezometric water significantly reduces slope stability, particularly for Slope 1 (Figure 6), which is highly susceptible to failure under wet conditions. Slope 2 remains stable due to higher cohesion and friction angle, while Slope 3 presents moderate stability. According to Griffiths & Lane et al., 1999; Liu et al., 2020 and Mebrahtu et al., 2022, slopes 1 and 3 are unstable.

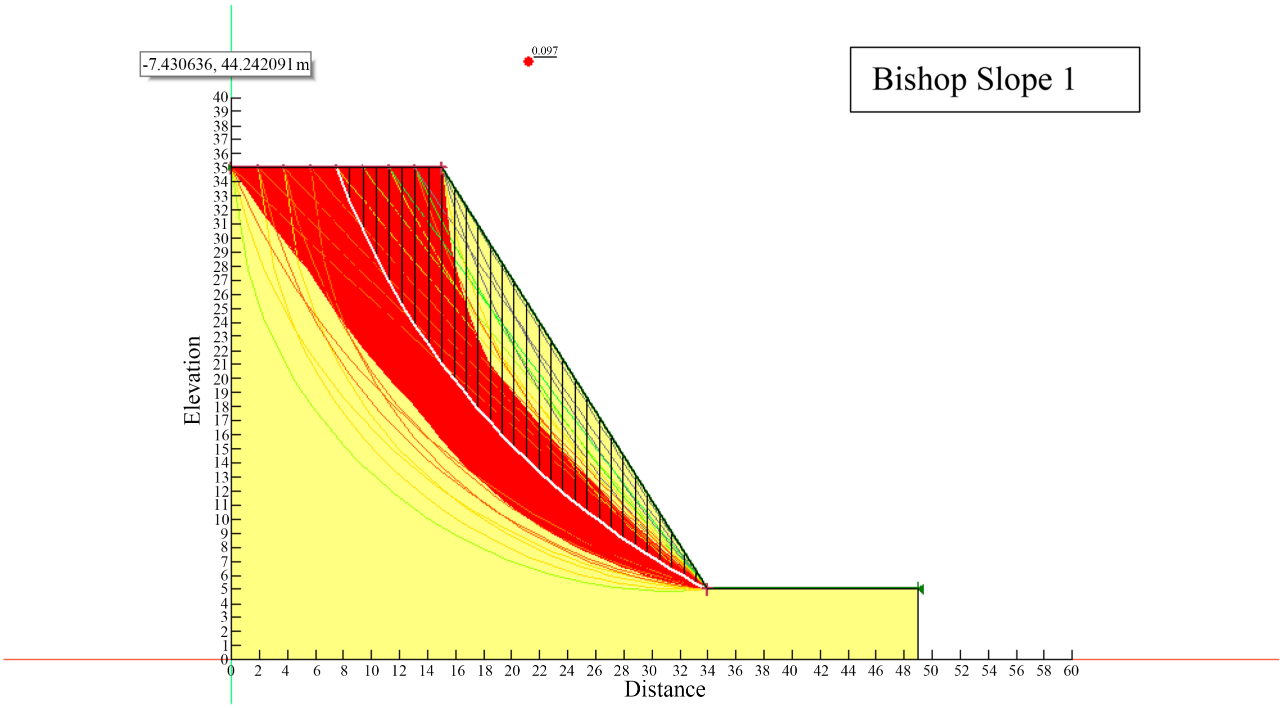

Figure 6. Factor of safety of slopes.

3.3.2. Slope Stability Using the Finite Element Method (FEM)

The main parameters used for the FEM analysis include the Young's modulus (E), Poisson's ratio (ν), oedometer modulus (E_oed), shear modulus (G), internal friction angle of the soil grains (φ), cohesion (C), and dilatancy angle (ψ). The numerical values of these parameters for the studied slopes are summarized in Table 10.

Table 10. Calculation parameters.

Parameter	Slope 1	Slope 2	Slope 3
Height H (m)	30.44	25	26.38
Slope β (˚)	59	52	23.76

Continued

Horizontal Distance D (m)	18.29	19.53	48
Young's Modulus E (kPa)	31705.05	21012.25	28933.42
Poisson's Ratio ν	0.32	0.29	0.34
Unit Weight γ (kPa)	15.79	15.96	15.21
Cohesion C (kN/m²)	24.03	70.44	54.8
Internal Friction Angle φ (˚)	31.85	19.53	28.77
piezometric water level (m)	5.4	2.12	2.41

3.3.3. Mesh, Boundary Conditions, and Deformations

The boundary conditions are selected in a standard manner. The mesh is of medium size. Figure 7 illustrates the mesh and the deformed mesh.

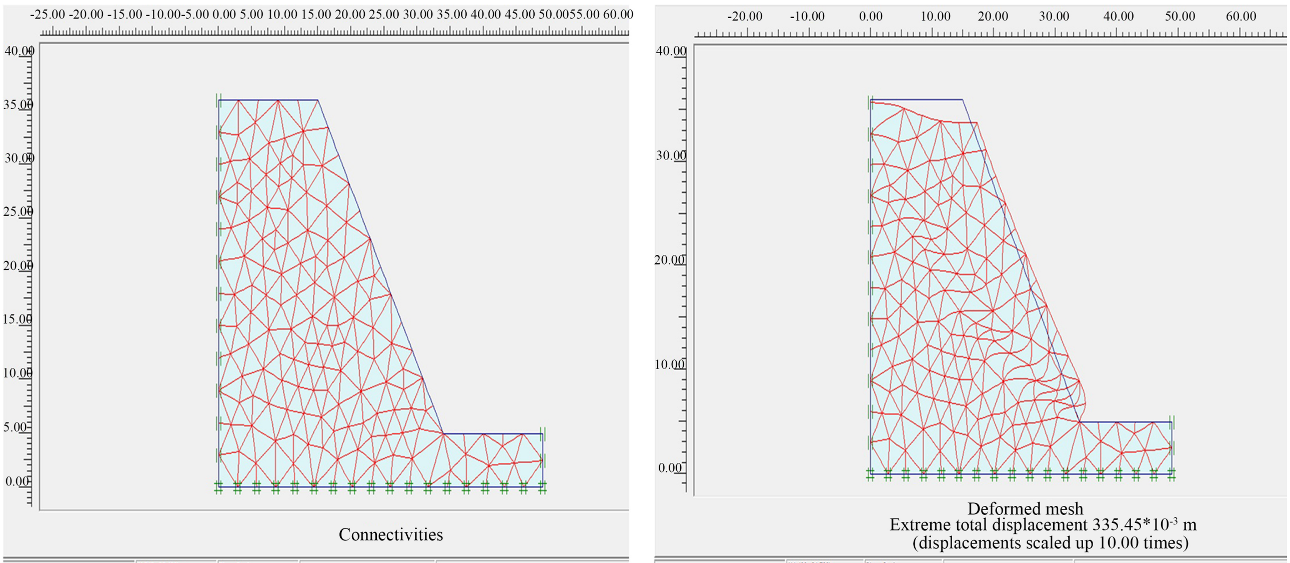

Figure 7. Meshes and boundary conditions; deformed meshes of the slopes.

The total displacement values for slopes 1, 2, and 3 are shown in Table 11. They are 0.335 m, 26.48 m, and 15.85 m, with corresponding factors of safety of 1.460, 3.815, and 3.146.

Table 11. Factor of safety (FS) and displacement results.

Slope	Slope 1	Slope 2	Slope 3
Displacement (m)	0.335	26.48	15.85
Factor of Safety (FS)	1.460	3.815	3.146

Table 12 presents the results of the factors of safety and displacements for the slopes under a defined piezometric water level.

The slopes 1, 2, and 3 have factors of safety (FS) of 1.460, 3.815, and 3.146, respectively. Slope 1 is considered marginally stable, whereas slopes 2 and 3 are stable, with corresponding maximum total displacements of 0.335, 26.48, and 15.85

m. Belazouz et al. (2024), in his study on the use of numerical methods for assessing the stability of earth dams in Algeria, reported FS values ranging from 1.458 to 54.45 (with displacements between 26.756 m and 50.08 m), which are much higher than those obtained in the present study, particularly with respect to displacements. This discrepancy may be attributed to differences in cohesion and internal friction angles. Regarding **Table 11**, the factors of safety range from 1.140 to 3.062, with displacements between 0.379 and 7.12 m. Liu et al., 2020 and Mebrahtu et al., 2022 also identifies slope 1 as marginally stable, while slopes 2 and 3 remain stable. The presence of water affects the soil parameters and contributes to a reduction in FS. Given the differences in FS values and the observed instability of slope 1 across both calculation methods, a comparative study of these methods is recommended, along with the construction and geotechnical monitoring of this slope.

Table 12. FS and displacement results with piezometric water level.

Slope	Slope 1	Slope 2	Slope 3
Displacement (m)	0.379	5.06	7.12
Factor of Safety (FS)	1.140	3.062	2.449

4. Comparative Study of Slope Stability Using FEM and LEM in Gouache and Surroundings

From **Table 13**, it is observed that the factors of safety (FS) obtained using the Finite Element Method (FEM) are higher than those calculated with the Limit Equilibrium Method (LEM). The FS values from LEM vary very little across the different hypotheses. This difference arises because LEM does not account for stress-strain relationships, considers fewer calculation parameters, does not compute displacements within the slope, and faces difficulties in simultaneously determining the critical slip surface, the normal and shear stresses along this surface, and the FS based on the failure criterion using equilibrium equations.

In contrast, FEM is capable of monitoring the progression of failure until completion, including global shear failure. Since no prior assumption is required regarding the shape or location of the failure surface, failure naturally occurs in regions of the soil mass where the shear strength is insufficient to resist applied stresses. As there is no notion of slices in FEM, no assumptions about lateral slice forces are needed. The FEM approach maintains global equilibrium until failure is reached.

Table 13. FS values from FEM and LEM.

Slope	LEM Ordinary	Bishop	Jambus	Spencer	Morgenstern-Price	FEM
1	0.965	0.997	0.939	0.967	0.966	1.460
2	2.125	2.173	2.135	2.177	2.173	3.815
3	1.655	1.701	1.654	1.702	1.698	3.146

Table 14 compares the safety factors (Fs) of the three slopes using the Limit Equilibrium Method (LEM) under various assumptions (Ordinary, Bishop, Jambus, Spencer, Morgenstern-Price) and the Finite Element Method (FEM). For all slopes, the Fs values obtained from FEM are consistently higher than those from LEM, reflecting FEM's ability to account for actual stress and deformation distributions as well as the natural progression of failure, whereas LEM relies on simplified assumptions regarding the slip surface and does not model displacements. Slope 1 is critical, with Fs < 1 in all LEM scenarios (0.760 - 0.840), indicating instability or marginal stability, while FEM yields a slightly higher Fs of 1.140, showing limited improvement but still a critical condition. Slopes 2 and 3 are stable under all methods, with FEM predicting substantially higher safety factors (3.062 for slope 2 and 2.449 for slope 3), highlighting the increased reliability of FEM. Variations between the different LEM assumptions are minimal, suggesting that while LEM provides a quick estimate of slope stability, it may underestimate the true safety compared to FEM, particularly when displacements and stress distributions are significant.

Table 14. FS values from FEM and LEM with piezometric water level.

Slope	LEM Ordinary	Bishop	Jambus	Spencer	Morgenstern-Price	FEM
1	0.840	0.764	0.760	0.760	0.761	1.140
2	1.867	1.773	1.742	1.781	1.770	3.062
3	1.442	1.395	1.360	1.398	1.395	2.449

5. General Conclusion

This study conducted a comparative analysis of slope stability in Gouache and its surroundings using the Finite Element Method (FEM) and Limit Equilibrium Methods (LEM). The objective was to assess, predict, and mitigate the risks of mass movement-related hazards. Field investigations included macroscopic soil description, sampling, and data collection. Laboratory tests comprised geotechnical characterization through identification tests (natural water content, specific gravity, Atterberg limits, and particle size distribution) and mechanical tests (Proctor compaction, CBR, drained shear, and oedometer tests).

Results indicate that the soils have low to medium plasticity, with a plasticity index averaging 18.6% (range: 14.63% - 23.07%). Maximum dry density at optimum Proctor ranged from 1.61 to 1.72 g/cm^3, optimum water content from 17% to 20.4%, and CBR at 95% OPM from 0.41% to 5.97%, reflecting very poor bearing capacity. Soils are predominantly clayey, classified as A-7-5 and A-7-6 (HRB), and low- to high-plasticity silts per Casagrande's chart. Cohesion values vary from 18.22 to 70.44 kPa, and internal friction angles from 28.74˚ to 36.7˚. Compressibility parameters indicate overconsolidation, with moderate to high compressibility.

Slope stability analysis showed safety factors ranging from 0.939 to 2.177 for LEM and from 1.406 to 3.815 for FEM, highlighting slope 1 as unstable, whereas slopes 2 and 3 are stable. Instability is primarily attributed to steep slopes, significant height, soil properties, water infiltration, and anthropogenic activity. These findings underscore the necessity of careful geotechnical monitoring and slope management to mitigate potential hazards.

Conflicts of Interest

The authors declare no conflicts of interest regarding the publication of this paper.

References

Belazouz, L., Bouzelha, K., Hammoum, H., Amiri, O., & Khelil, N. (2024). Reliability Analysis of the Slope Stability of Homogeneous Earth Dam under Seismic Loading. *Periodica Polytechnica Civil Engineering, 68,* 107-121. https://doi.org/10.3311/ppci.22537

Griffiths, D. V., & Lane, P. A. (1999). Slope Stability Analysis by Finite Elements. *Géotechnique, 49,* 387-403. https://doi.org/10.1680/geot.1999.49.3.387

Kusumajaya, A. A. N., Mubasyiroh, R., Sudikno, S., Nainggolan, O., Nursanyoto, H., Sutiari, N. K. et al. (2023). Sociodemographic and Healthcare Factors Associated with Stunting in Children Aged 6 - 59 Months in the Urban Area of Bali Province, Indonesia 2018. *Nutrients, 15,* Article 389. https://doi.org/10.3390/nu15020389

Liu, S., Su, Z., Li, M., & Shao, L. (2020). Slope Stability Analysis Using Elastic Finite Element Stress Fields. *Engineering Geology, 273,* Article 105673. https://doi.org/10.1016/j.enggeo.2020.105673

Mebrahtu, T. K., Heinze, T., Wohnlich, S., & Alber, M. (2022). Slope Stability Analysis of Deep-Seated Landslides Using Limit Equilibrium and Finite Element Methods in Debre Sina Area, Ethiopia. *Bulletin of Engineering Geology and the Environment, 81,* Article No. 403. https://doi.org/10.1007/s10064-022-02906-6

NF P94-050. (1995). *Détermination de la teneur en eau pondérale des matériaux-Méthode par étuvage* (8 p). AFNOR.

NF P94-054 (1991). *Sols: Reconnaissances et essais, Détermination de la masse volumique des particules solides des sols, Méthode du pycnomètre à eau.* Association Française de Normalisation, France. (In French)

NF P94-056 (1996). *Analyse granulométrique: Méthode par tamisage à sec après lavage* (16 p). AFNOR.

NF P94-071-1 (1994). *Essai de cisaillement rectiligne à la boite* (16 p). AFNOR.

NF P94-090-1 (1994). *Réalisation de l'essai odométrique* (24 p). AFNOR.

Tahar, R., & Mouatez, B. (2023). *Analyse de la stabilité des terrains en pente: Etude comparative.* Doctoral Dissertation, Université Echahid Chikh Larbi Tebessi-Tebessa.

Tsoata, F. T., Yemmafouo, A., & Ngouanet, C. (2020). Cartographie de la susceptibilité aux glissements de terrain à Bafoussam (Cameroun). Approche par analyse multicritère hiérarchique et Système d'information géographique. *Revue internationale de géomatique, 7,* 1-31.

Zangmene, F. L., Ngapna, M. N., Ateba, M. C. B., Mboudou, G. M. M., Defo, P. L. W., Kouo, R. T. et al. (2023). Landslide Susceptibility Zonation Using the Analytical Hierarchy Process (AHP) in the Bafoussam-Dschang Region (West Cameroon). *Advances in Space Research, 71,* 5282-5301. https://doi.org/10.1016/j.asr.2023.02.014